Tests of local transport theory and reduced wall impurity influx with highly radiative plasmas in the Tokamak Fusion Test Reactor

K. W. Hill, S. D. Scott, M. Bell, R. Budny, C. E. Bush,[1] R. E. H. Clark,[2] B. Denne-Hinnov, D. R. Ernst, G. W. Hammett, D. R. Mikkelsen, D. Mueller, J. Ongena,[3] H. K. Park, A. T. Ramsey, E. J. Synakowski, G. Taylor, M. C. Zarnstorff, and the TFTR Group

Princeton Plasma Physics Laboratory, P. O. Box 451, Princeton, NJ 08543

Abstract

The electron temperature (T_e) profile in neutral beam-heated supershot plasmas (T_{eo} ~ 6 - 7 keV, ion temperature T_{io} ~ 15 - 20 keV, beam power P_b ~ 16 MW) was remarkably invariant when radiative losses were increased significantly through gas puffing of krypton and xenon in the Tokamak Fusion Test Reactor (TFTR) [K. M. McGuire *et al.*., Phys. Plasmas 2 (1995) 2176]. Trace impurity concentrations ($n_Z / n_e \sim 10^{-3}$) generated almost flat and centrally peaked radiation profiles, respectively, and increased the radiative losses to 45 - 90% of the input power, (from the normal ~25%). Energy confinement was not degraded at radiated power fractions up to 80%. A 20 - 30% increase in T_i, in spite of an increase in ion-electron power loss, implies a factor of ~3 drop in the local ion thermal diffusivity. These experiments form the basis for a nearly ideal test of transport theory, since the change in the beam heating power profile is modest, while the distribution of power flow between (1) radiation and (2) conduction plus convection changes radically and is locally measurable. The decrease in T_e was significantly less than predicted by two transport models and may provide important tests of more complete transport models. At input power levels of 30 MW, the increased radiation eliminated the catastrophic carbon influx (carbon "bloom") and performance (energy confinement and neutron production) was improved significantly relative to that of matched shots without impurity gas puffing.

PACS: 52.55.-S, 52.55.Fa

[1] Oak Ridge National Laboratory, Oak Ridge, TN

[2] Los Alamos National Laboratory, Los Alamos, NM

[3] Laboratoire de physique des plasmas, Ecole royale militaire, Brussels, Belgium

I. INTRODUCTION

Two of the most challenging problems in tokamak magnetic fusion research are (1) solving the problem of heat flow onto the first wall[1,2,3,4,5,6,7,8] and (2) both understanding and finding a way to control anomalous transport.[9,10,11,12,13,14,15,16,17,18,19,20,21] In a reactor several hundred megawatts of alpha heating power will have to be exhausted, mainly onto the divertor plates, possibly leading to excessive heat loading,[1-8] erosion, and production of impurities which can degrade the nuclear reactivity. One of the most promising solutions proposed for this problem is the use of impurity radiation associated with controlled gas puffing to remove a substantial portion of the thermal energy. This technique reduces the concentrated heat flux density at the divertor or limiter.[1,22,23,24,25,26] This scheme has been called the radiative "mantle" or highly radiative plasma. To minimize the size and cost of a reactor, yet be sure of achieving ignition with a comfortable margin, understanding thermal transport is important, because reactor design requires extrapolating from present, smaller experiments. The extrapolations can be reliable only if the plasma models used are reliable. Also, understanding transport mechanisms may enable experimental attainment of advanced tokamak regimes which can improve performance and lead to more efficient and cost effective reactor designs.[27] Extensive research, both theoretical and experimental, has been done on both the transport issue[9-20] and the question of dissipating the fusion power by impurity radiation.[1-8,28,29,30,31] In this paper the approach of using feedback controlled impurity radiation is discussed. This technique is used to study both the thermal transport and the potential for reduction of thermal loading of the first wall.

This paper reports the first successful use of controlled high-Z (krypton and xenon) gas puffing at reactor-plasma conditions to increase, by factors of two to three, the fraction of input power which is removed by radiation. Results from two distinct types of experiments are reported. These are (1) high neutral beam power (P_B>28 MW) discharges in which the intense impurity influxes from the graphite limiter (carbon "blooms"),[32,33] often seen without impurity puffing, were successfully suppressed by impurity puffing, and (2) modest power (16 - 22 MW) shots for transport studies; here the lower beam power was used to avoid carbon "blooms" and to minimize MHD activity which can affect transport. A remarkable observation is that this large increase in radiated power was accomplished without degrading plasma confinement or fusion power production in the transport-study experiments. In the higher power bloom-suppression studies, both confinement and fusion power output were improved relative to that in matched shots with no impurity gas puff. The advantage of removing power by radiation is that the power is deposited uniformly to the vacuum vessel wall. In contrast, power which is conducted or convected to the limiter or divertor is concentrated onto a much smaller area, leading to much higher heat loading per unit area. The reduced limiter heat loading brought about by the high-Z radiation prevented uncontrolled carbon influxes at high heating power (P_b ~ 30 - 40 MW), thereby improving confinement and fusion power by reducing the "rollover" or degradation of these parameters with time. Thus, further development of this technique could greatly ameliorate or even solve the problems of heat loading to divertors and concomitant uncontrolled wall impurity release.

Previous work on highly radiating plasmas has generally involved impurities with lower atomic number, such as N, Ne, and Ar for increasing the radiative losses in both the main plasma and the divertor region, and much of this work has been done at temperatures well below the reactor regime.[7,34,35,36,37] The present study extends the work to higher-Z ions such as Kr and Xe in reactor-regime plasmas with central electron and ion temperatures T_{e0} = 6 - 9 keV and T_{i0} = 15 - 40 keV. Most of the studies were done in the supershot regime.[38] The higher-Z ions were more effective in TFTR for radiating multi-megawatt levels of power with minimal dilution of the deuterium or tritium fuel ions. It has been shown[39] that at electron temperatures in the range from 100 eV to about 10 keV, typical of future reactors or large tokamaks, the radiated power increases very strongly with Z. The effective plasma fuel-ion dilution, which is proportional to the average charge of the impurity ions, increases much more weakly. Thus, high-Z radiators can provide the required radiative cooling with much lower impurity ion densities and, thus, lower dilution than lower-Z impurities.

This paper also reports on further tests of transport theories by analyzing the plasma response to the high-Z impurity puffing. The highly radiative plasmas provide a nearly ideal method to test thermal transport because the changes in the distribution of power flow between radiation and conduction plus convection are large and are locally measurable by bolometry, while changes in the electron density and neutral-beam deposition profile are relatively small. As discussed in Sec. IV, the small change in T_e accompanying the large increase in radiative power loss from the electrons is very likely a result of compensation of the increased radiative losses by an increased power flow to the electrons from the ions. The small change is T_e is also consistent with the TRANSP analysis of Sec. V, which shows that the net power flow in the electron channel is nearly unchanged with the large increase in radiative losses in the impurity puffing shots.

In the transport experiments the core electron density n_e was found to increase by 15 - 30% with the increased radiation. The ion temperature T_i was also significantly increased. The increase in density suggests an improvement in particle confinement, since (1) the edge source due to recycling of deuterium was actually reduced, and (2) the increase in electrons due to the impurity gas which entered the plasma was much smaller than the observed increase in electron density. The increase in ion temperature was remarkable because a larger fraction of the ion energy was being coupled to the electrons due both to the increased density and to the increased ion temperature [ion-electron equilibration power $q_{ie} \sim n_e^2 (T_i - T_e) / T_e^{3/2}$]. These observations provide further information for testing transport models.

In Sec. II the experimental technique and phenomenology of the highly radiative plasmas are described. In Sec. III high heating power experiments are described in which the high-Z radiation was used to reduce the power flowing to the limiter and prevent uncontrolled carbon influxes. In Sec. IV the more modest power transport experiments are discussed, and in Sec. V the results of a transport analysis of a xenon-puffing experiment are presented.

II. PRODUCTION OF HIGHLY RADIATIVE PLASMAS

The highly radiative plasmas were produced by injection of the noble gases Ar, Kr, and Xe into supershot plasmas. The effects of the puffing are illustrated in Fig. 1. Basic plasma conditions for these shots were R=2.52 m, a=0.87 m, B_t=4.75 T, I_p=2.0 MA, q_{psi}=4.6, P_b = 16.6 MW, P_{co}/P_b = 0.7, where the parameters are R: major radius, a: minor radius, B_t: toroidal field strength, I_p: plasma current, q_{psi}: inverse rotational transform at the plasma edge, P_b: neutral beam heating power, and P_{co}: power of neutral beams injecting tangentially in the direction of the plasma current. Prior to these discharges the limiter was prepared in the usual fashion[40] needed to ensure supershot plasma operation, including a sequence of Ohmic helium plasmas. The plasma density was sustained almost entirely by hydrogen influx from the limiter surface and beam fueling. In the Kr experiments, no gas other than Kr was puffed during the discharges; the Xe was diluted to about 20% by deuterium. The D influx from puffing the mixture was negligible relative to the fueling from the wall. All characteristic features of the supershot plasma regime were realized: enhanced global energy confinement, τ_E = 135-155 ms = 1.3-1.5 times $\tau_{E\text{-}89P}$,[41] low edge density and a peaked density profile, n_{e0} / $<n_e>$ = 2.05-2.45, modest line-average density $n_e = 2.8\text{-}3.4 \times 10^{19} m^{-3}$, and high central ion temperatures T_{io} = 20-24 keV and T_{io}/T_{eo} = 3-4.

The gas puffing rate was feedback controlled on the measured radiated power fraction $f_R = P_{RAD}/(P_{NBI} + P_{OH})$ by means of a digital computer. Here P_{RAD}, P_{NBI}, and P_{OH} are the total radiated power, the neutral-beam heating power, and the Ohmic heating power, respectively. Figure 1 illustrates the results of puffing xenon into plasmas at two different rates. Shown are the deuterium neutral beam heating power P_b of 16 MW, which was injected from 3.0 to 5.0 s, the radiated powers for the three shots, and the requested gas injection rates of the two shots with gas puffs. These puff rates were set to sustain radiated power fractions of 45% and 75% from t = 3.5 s to 4.6 s for the shots illustrated by curves with long dashes and short dashes, respectively. The requested gas puffing rate first increased to high values, since the measured radiated power fraction was well below the requested value, and then decreased to a steady-state value as the measured power fraction approached the target. It was found, in agreement with experience on TEXTOR[42] , that such feedback control of the gas puff rate was essential for obtaining steady state plasmas with high radiative power fractions. This requirement is presumably due to the nonlinear dependence of the gas penetration, recycling, and radiation on puff rate because of modification of edge plasma parameters by the puff. Without feedback control, attempts to increase the radiated power by increasing the gas flow rate would often lead to disruption. We also see from Fig. 1 that the energy confinement time τ_E was essentially unchanged or even slightly improved by the xenon puffing, relative to that of the no-puff shot, but that the deuterium influx, which is approximately proportional to the Dα emission shown, was substantially reduced. A reduction in deuterium influx usually correlates with improved confinement in supershots,[43] all other parameters being the same.

The plasma concentration (ion density n_I / n_e) of the injected impurity gas ions was very small, resulting in low dilution of the fuel ions. A knowledge of this concentration is important for further modeling and understanding of the highly-radiative experiments.

The impurity concentration was estimated from the increase in Z_{eff} due to the impurity, with an assumed uncertainty of ± 35% ($n_I/n_e = \Delta Z_{eff} / \langle Z \rangle^2$, where <Z> is the average charge state predicted by the MIST impurity transport code[44,45]). The uncertainty derives from uncertainties in the calibration, the Abel inversion, the estimate of <Z>, and subtraction of two Z_{eff} values. For a shot with xenon puffing and 75% radiated power, the inferred concentration was (7.2 ± 2.5) x 10^{-4}, for a fuel dilution value ($\Delta n_H/n_H$) in the core of 3.0 ± 1.0%. For a shot with krypton puffing and 85% radiated power the inferred concentration was (1.46 ± 0.5) x 10^{-3}, translating to a fuel dilution in the center of 4.6 ± 1.6%. For both krypton and xenon the concentration profile was approximately flat from r/a = 0 to r/a = 0.7. For krypton additional estimates of the concentration were inferred near r/a = 0.7 from the intensity of (1) the Na-like VUV resonance line at 179 Å, (1.4 x 10^{-3}), (2) the Mg-like VUV resonance line at 158 Å (7.3 x 10^{-4}), or at r/a = 0 from (3) the soft x-ray K resonance peak near 13 keV (2.9 x 10^{-3}).[46] These measurements are in reasonable agreement with the estimates from the increase in Z_{eff}, considering the uncertainties in the spectroscopic modeling. The higher estimate from the x-ray diagnostic is not surprising, since it is impossible to include in the theoretical atomic model contributions to the effective excitation rate from all of the many hundreds of excitation channels. These include contributions from excitation to n>2 levels followed by cascading and contributions from many dielectronic-recombination configurations.[47]

Only trace levels of the xenon puffed into the shots of Fig. 1 entered the plasma. Approximately 9 Torr-liters of xenon gas were puffed into the torus. The electrons associated with this quantity of gas correspond to ~20 times the total electron population in the plasma, and would represent an electron source rate 11 times higher than the electron source rate due to ionization of deuterium gas evolved from the limiter surface as measured by Dα light emission. Nevertheless, the xenon concentration in these plasmas, as estimated from the measured increase in Z_{eff} of ~ 1, remained very small (n_{Xe}/n_e = 0.72 x 10^{-3}, hydrogenic ion dilution = n_{Xe}/n_e <Z> approximately 0.03). Here <Z> is the average charge of the xenon ions, which is predicted by the MIST code to be 42 in the center of the discharge. The edge electron density as measured by a vertically-viewing interferometer at R=1.80 m (r/a=0.83) changed less than 5% between the xenon and no-xenon discharges. We conclude that only a small fraction of the puffed xenon enters the plasma; the remainder is presumably entrained in the limiter[48] or vacuum-vessel surfaces during the plasma discharge and is then pumped away in the 10-15 minute period between discharges. Bolometric and spectroscopic diagnostics on reference discharges, following discharges with impurity-Z gas puffing, showed a rapid decrease in the high-Z impurity concentration (typically a factor ~3-5 decrease on the first shot), indicating that there is little long-term accumulation of these gases in the limiter.

The local increases in radiated power due to the injected impurity gases ranged up to factors of 6 in the steady-state experiments, and a range of radiated power profiles[49,50] were achieved by injecting different gases, as shown in Fig. 2. This local increase is larger than the factor of 2-3 increase in the global radiation. These large increases in local radiation enabled rather strong tests of transport theories. In the reference shot of Fig. 2 with no impurity puff, the radiation is edge dominated and is mainly due to lines from carbon ions which are not fully stripped near the edge. The argon radiation is also concentrated near the edge, but is much higher in magnitude than the carbon radiation. Both krypton and xenon radiate across the entire plasma, with the krypton radiation slightly hollow and the xenon radiation slightly peaked in the center.

The profiles in Fig. 2 are derived from a poloidal average of tomographically reconstructed data from two bolometer arrays, one radially viewing and the other vertically viewing the plasma. These shots had similar parameters to those of Fig. 1, except for the shot with argon puffing, which had a neutral-beam heating power of 22 MW. The total radiated power for the shots ranged from about 75% to almost 100% of the neutral-beam power.

III. REDUCTION OF LIMITER HEAT LOADING AND IMPURITY INFLUXES

One of the most encouraging outcomes of the highly radiative plasma experiments with high power neutral-beam heating (P_B > 28 MW) was the successful suppression of large influxes of impurities from the limiter ("blooms")[32], with a resulting improvement in performance. During previous experiments at high power, the blooms had often led to a severe reduction or "rollover" in confinement and neutron production and had severely limited the duration, and probably the maximum fusion power output, of the high power phase of the discharges.[32] The improved performance with the high-Z radiation resulted in a record value of total fusion energy production being achieved during the radiative experiments (new record, 7.6 MJ; previous record, 6.5 MJ[51]). The record was achieved even though the machine was in a considerably poorer state of conditioning (with respect to removal of deeply embedded deuterium in the graphite tiles from L-mode operation and clean-up of intrinsic impurities following disruptions)[42,52,53] during these experiments, than during earlier high power, high performance DT experiments.[54]

Successful suppression of carbon blooms and improvement of confinement and neutron production are illustrated in Fig. 3. The time histories of two shots with R=2.52 m, a=0.87 m, B_t= 5.1 T, I_p=2.2 MA, and P_b = 30 MW from t = 2.8 - 4.6 s are shown. In the shot without the xenon puff the total radiated power was about 8 MW, or 27% of the heating power, rising to 8.8 MW at the end of the NBI (neutral-beam injection) phase. The remaining 22 MW of the heating power was conducted or convected to the edge, leading to an increase in carbon influx (carbon "bloom") from the limiter which is proportional to the CII brightness shown in Fig. 3b.[55,56] The energy confinement time τ_E dropped to 82 ms, or 94 % of L-mode. In the shot with the xenon puff from 2.9 to 4.4 s, as shown in the first frame, the additional 6 - 7.6 MW of xenon radiation reduced the power to the limiter to about 15 MW. The carbon bloom disappeared, τ_E remained 20-40% higher, and the fusion power (DD neutron production rate) increased by 30 - 40%.

Local reductions in the CII brightness by high-Z impurity gas puffing were often much larger than the factor of 2 shown in Fig. 3 (b). This signal is the average of intensities of the 6585Å line from nine filter/fiber telescope channels[57] viewing the limiter at different poloidal locations. Without the xenon puff the signal from a single CII channel viewing the limiter at 17° below the midplane, as measured from the center of the vacuum vessel, was unusually high and dominated the total CII brightness, indicating that its field of view included localized emission from a hot spot on the limiter. With the xenon puff the intensity of the signal from this channel was reduced by a factor up to 7. In other high power shots emission from such local hot spots was even more dominant, and was reduced by factors as large as 14 by the high-Z gas puffing. Other parameters which were higher in the no-puff discharge shown in Fig. 3 and the maximum factors by which they were higher are the near-edge electron density, 1.9; a central line-integrated electron density, 1.4; the total number of electrons in the discharge, 1.5; the central electron density $n_e(0)$, 1.1. The electron density peaking factor $n_e(0)/\langle n_e \rangle$ was lower by a factor 0.70 in the no-puff shot, where $\langle n_e \rangle$ is the volume averaged electron density.

IV. TRANSPORT EXPERIMENTS

A surprising result of the experiments with krypton and xenon puffing is that the plasma temperatures did not decrease significantly when the core radiation was increased by such large factors. The behavior of the temperatures is illustrated in Fig. 4 for xenon puffing to a radiated power fraction of 75%. The shots in this figure are typical of the plasmas which were used in the transport studies. The radiated power was increased by a factor of 3 globally, but a factor of 6 in the center due to the xenon (see Fig. 2), yet the central T_e dropped at most about 15% relative to that of the reference shot. Naively one would expect a much larger drop in T_e to accompany such a large increase in the power-loss term of the electrons. The increase in central electron density implies improved particle confinement, since the increase is much larger than the increase in electrons from the xenon ($n_i/n_e <Z> \sim 7.2 \times 10^{-4} \times 42 \sim 0.03$), the beam fueling did not change, and the edge fueling decreased significantly as shown in Fig. 1 (d). We also see that the total stored energy in Fig. 4 and, thus, the energy confinement time was actually higher in the shot with xenon puffing (dashed curves) than in the reference shot without xenon. Intuitively one might expect that the stored energy might be lower in the shot with xenon since the radiative power loss from the center of the plasma is higher by a factor approaching 6 (see Fig. 2). Also shown in the figure are an increase in the DD neutron emission rate S_{DD}, and central electron density. With the xenon puff the ion temperature increased above its value in the reference shot and remained higher. The increase in neutron emission is consistent with the higher ion temperature, and also consistent with the small deuterium dilution discussed in Sec. II. The large increase in ion-electron equilibration power q_{ie} can explain the lack of decrease in T_e, since it compensates for the increased radiation losses.

In the modest-power transport studies either no change or a very small change in global energy confinement time τ_E occurred with enhanced radiative losses from puffing of argon, krypton, or xenon gases. The confinement results are summarized in Fig. 5, which plots the ratio of global τ_E [$= W_{tot}/(P_{OH} + P_b - dW_{tot}/dt)$] in supershot discharges with high-Z impurity puffing to matched reference discharges without puffing. All data points not connected by a line represent quasi-stationary discharge conditions for which the dW_{tot}/dt term contributes less than 15% to τ_E. The thin line connecting four Ar points and the thick line for Kr each represents a single shot that ultimately suffered radiative collapse. The global τ_E was remarkably insensitive to the additional radiative losses, e.g.,

τ_E decreased less than 5% for both xenon and krypton at radiated power fractions up to 75% and 100% respectively. Limited experience with argon showed a deterioration of 15-20% at high radiated power fraction (f_R > 85%). The absence of a drop in τ_E accompanying the large increase in radiative power loss is likely related to the reduced deuterium recycling seen in Fig. 1(d).

V. RADIAL PROFILES AND TRANSP ANALYSIS RESULTS

Radial profiles of several parameters for the radiative versus non-radiative comparison shots from Fig. 4 are shown in Fig. 6. These profiles are either measured input parameters or derived parameters calculated by the TRANSP code.[57] The solid curves are for the shot with no gas puff, and the dashed curves are for the matched shot with a xenon puff. In some frames a third, dotted, curve is shown which represents the TRANSP calculation run in predictive mode for a fictitious plasma having the measured beam deposition, radiation, and density profiles from the xenon-puff shot, but using the conductivities (χ) inferred from the no-xenon shot. Thus, these curves represent the temperatures, etc. predicted for the shots with a Xe puff, assuming that the relevant conductivities did not change with the gas puff.

We see from Fig. 6 that the total net heating power did not change across the profile, except for a small increase near the center of the discharge. The electron density increased, particularly in the center, by a factor much larger than the ~ 3% increase expected due to the electrons from the Xe ions; this increase suggests a ~20% increase in particle confinement, particularly since the influx of both deuterium and carbon decreased with the Xe puff.

The curves labeled q_{rad} in Fig. 6 show that with the xenon puff the radiated power density increased across the entire profile by a factor as high as 6. This increase integrates to an increase in the overall power loss term to the electrons from 25% to 75%, or a factor of 3, as shown previously in Fig. 4.

The naive expectation for the plasma's response to increased radiative losses from xenon is reduced electron temperature, since less power should be available to sustain T_e against conduction. The actual plasma response was complicated by two unexpected factors: an apparent improvement in core particle confinement [higher $n_e(0)$] and a significant improvement in core ion energy confinement (higher T_{io}). These effects greatly increased the ion-electron equipartition power in the plasma core (R/a < 0.5), ΔP_{ie} = 3.00 - 0.84 = 2.16 MW, which nearly offsets the increased radiation, ΔPrad = 2.94 - 0.64 = 2.30 MW. The observation that the core electron energy content remained nearly constant with xenon puffing (W_e(r/a < 0.5) = 0.41 versus 0.42 MJ) thus reflects an underlying electron thermal conductivity χ_e that is unchanged in the presence of xenon. The total electron energy content of the plasma went from 0.62 to 0.61 MJ.

Figure 6 shows that the core χ_e inferred from kinetic power-balance analysis is very similar between the xenon and no-xenon discharges. Figure 6 also illustrates the expected T_e response (dotted curves) in the xenon discharge given a χ_e that remains fixed at the magnitude and profile inferred without xenon, but taking all other conditions (n_e, T_i, heating profile, Z_{eff}, P_{OH}) from the measured parameters of the xenon discharge. A net small decrease in T_e is expected over the profile. The actual decrease in T_e was slightly larger than expected in the plasma center and smaller than expected in the plasma periphery, the latter reflecting somewhat improved χ_e in the edge of the xenon discharge.

In the absence of xenon puffing, the electron power balance in the plasma core (volume-integrated to r/a = 0.5) is dominated by collisional beam heating (68%) with smaller contributions from Ohmic heating (7%) and ion-electron equilibration (26%); the losses are conduction plus convection (80%) and radiation (20%). When xenon is added, the increase in radiative losses (2.3 MW) is almost balanced by the increased ion-electron equilibration power (2.2 MW). With xenon, the electron power balance is ion-electron equilibration (52%), collisional beam heating (40%), and Ohmic heating 7%), and the losses are conduction plus convection (45%) and radiation (51% plasma core, r/a < 0.5).

The most remarkable plasma response to the increased radiative losses is the increase in ion temperature. The increase in n_e and T_i result in a factor of 2 increase in ion stored energy. If the ion thermal conductivity χ_i had remained unchanged, the ion temperature should have dropped by a factor approaching 2 in the center, as shown by the TRANSP predicted dotted curve. The actual increase in T_i and the modest drop in T_e, as well as the increased electron density, contribute to an increased ion-electron equilibration term (Fig. 4), which modifies both the net electron and ion heating; the q_{ie} becomes an extra heating term for the electrons and a loss term for the ions. Thus, the net heat flow through the electron channel Q_e with xenon puffing is larger in the core and smaller for $x > 0.5$, and that for the ions Q_i is smaller throughout the plasma. The increase in ion temperature, in spite of the greatly increased loss from the ion-electron equilibration power, is interpreted as a significant decrease in ion thermal conductivity χ_i.

The plasma rotation velocity Ω_ϕ also increased with the Xe puffing, resulting in a net decrease in the momentum diffusivity χ_ϕ. If this diffusivity had not changed with the puffing, the rotation velocity would have changed only slightly, as illustrated by the dotted curve.

The measured electron- and ion-temperature profiles from supershots in the modest power (P_B=16 MW) transport studies were compared with predictions of two transport models. These were the IFS-PPPL[14] model and the RLWB (Rebut-Lallia-Watkins-Boucher) model[58]. One goal of the comparisons was to understand the small change in the measured electron temperature (Fig. 6) accompanying the large increase in radiative losses to the electrons. The temperatures were predicted by solving the power-balance equations using the neutral-beam and Ohmic heating powers, the radiative losses, and electron and ion densities from the TRANSP code as described in Ref. 21. Both models greatly overestimated (factor of 2) the drop in T_e with the xenon puff and, therefore, agreed more with the naively expected change.

These differences between the predicted and measured response of the temperatures to the greatly increased radiated power are not surprising because the models' predictions were not in accord with the low radiation supershots. It is hoped that the discharges described in this paper will provide an important test of a more complete model which does adequately predict the temperatures in the low radiation shots.

VI. DISCUSSION

The influence of the q profile evolution on the confinement evolution was considered, but no firm conclusions about this effect could be established. It has been suggested that the slower downward evolution of τ_E seen in Figs. 1 and 4 might be connected to the evolution of the q profile, since this evolution might be different in the highly radiative shots because of the higher Z_{eff} (ΔZ_{eff} ~1) . Unfortunately, measurements of the q profile were not available for the discharges studied in this paper.

However, TRANSP calculations of q showed that the change in q during the gas puff for the shot of Fig. 4 differed from that over the same time interval in the no-puff shot by less than ±2% for $r/a \geq 0.2$. In the center, q increased more rapidly in the gas puff shots than in those without gas puffing. The relative increase was 20, 20, and 8% higher at r/a = 0.05, 0.1, and 0.15, respectively. Thus, TRANSP calculated a significantly different q profile evaluation (8-20%) during the gas puff only in the center of the plasma ($r/a \leq 0.15$).

It was confirmed by separate calculations that the effect of the xenon in the plasma on the neutral beam stopping was adequately approximated by TRANSP. In TRANSP the presence of one or more impurities in the plasma is treated by assuming a single impurity having a specified Z, and calculating the impurity density from the measured Z_{eff} . In the present study, the same constant impurity Z was assumed for both the highly radiative shots and the discharges without high-Z gas puffing (although the effective impurity density was higher in the Xe puffing shot because of the higher Z_{eff}). In a separate study the beam stopping was calculated for a plasma having the same Z_{eff} as a Xe-puff shot, but assuming that the Z_{eff} - 1 resulted from carbon only. For comparison, the stopping was calculated for a plasma with the same Z_{eff}, but assuming a mix of C and Xe, with the C density being the same as that in a reference shot without Xe puffing. The beam stopping at r/a = 0.5 for the latter, "correct" case was only 2% lower than that calculated assuming that the Z_{eff} - 1 resulted from C only. Thus, a very small error in the neutral beam stopping results from the fact that TRANSP was not aware that the additional impurity was Xe.

In summary, the study of highly radiative plasmas for heat dispersal has been extended to reactor relevant regimes in TFTR by controlled injection of trace levels of the high-Z gases krypton and xenon. Up to 50-75% of the heating power could be exhausted by radiation without deleteriously affecting plasma performance, as determined by energy confinement, neutron production, and plasma temperatures. With krypton injection, influxes of impurities from the limiter, particularly carbon, were greatly reduced in high performance supershots with neutral beam heating powers > 28 MW, resulting in significant improvements in confinement and DD neutron production, relative to the levels in matched shots without impurity gas injection. Also, krypton injection enabled longer sustainment of DT fusion power production at the several MW level, integrating to a DT fusion energy of 7.6 MW. This was an increase of 1.1 MJ from the old TFTR record value, even though the level of limiter conditioning in the present experiments was significantly inferior to that during the earlier experiments without increased radiative exhaust of heat. These experiments suggest a path toward significant reduction in divertor and/or wall heat loading in tokamak reactors. In modest power (P_{NB} = 16 - 22 MW) plasmas for transport studies, tripling of the radiative power (from the normal 25% to about 75%) resulted in very little change in T_e or energy confinement and a significant increase in n_e and T_i. The higher ion-electron equipartition energy compensated for the greatly increased radiative losses to the electrons, to result in very little change in T_e. Preliminary comparisons of the change in T_e and T_i to predictions of two transport models were made. Both models predicted a much larger decrease in T_e, than the measured decrease, in the highly radiative plasmas, relative to that in matched plasmas without the increased high-Z impurity radiation. It is hoped that comparisons of the experimental results with predictions of a more complete model which more accurately describes the reference plasma, without additional radiation, will lead to improvements in understanding of thermal transport.

ACKNOWLEDGMENTS

The authors gratefully acknowledge the support and encouragement of Drs. R. Hawryluk and K. McGuire. This work was supported by U.S. DoE Contract No. DE-AC02-76CH03073.

REFERENCES

[1] M. Ali Mahdavi, G. M. Staebler, R. D. Wood, D. G. Whyte, and W. P. West, J. Nucl. Mater. **241-243**, 305 (1997).

[2] G. Janeschitz, K. Borass, G. Federici, Y. Igitkhanov, A. Kukushkin, H. D. Pacher, G. W. Pacher, and M. Sugihara, Journ. of Nucl. Mater. **220-222** (1995) 73.

[3] D.E. Post, ITER Doc. Series No. 21 IAEA, Vienna, Austria (1991)

[4] G.C. Vlases, Plasma Phys. **35** (1993) B67

[5] P. Monier-Garbet, J. Nucl. Mater. **241-243**, 92 (1997)

[6] H.-S. Bosch, D. Coster, R. Dux, C. Fuchs, G. Haas, et al., J. Nucl. Mater. **241-243**, 82 (1997)

[7] G. Vlases, G. Corrigan, and A. Taroni, J. Nucl. Mater. **241-243**, 310 (1997)

[8] A. Kallenbach, H.-S. Bosch, S. de Pena Hempel, R. Dux, M. Kaufmann, et al., Fusion Eng. Des. **36**, 101 (1997)

[9] K. L. Wong , N. L. Bretz , T. S. Hahm, E. Synakowski, Phys. Letters A **236**, 339 (1997)

[10] J. A. Wesson, B. Alper, A. W. Edwards, and R. D. Gill, Phys. Rev. Lett. **79**, 5018 (1977)

[11] C. M. Greenfield , D. P. Schissel, B. W. Stallard, E. A. Lazarus, G. A. Navratil , et al., Phys. Plasmas **4**, 1596 (1997)

[12] F. Wagner and U. Stroth, Plasma Phys. Control. Fusion **35**, 1321 (1993)

[13] J. W. Connor and H. R. Wilson, Plasma Phys. Control. Fusion **36**, 719 (1994)

[14] M. Kotschenreuther, W. Dorland, M. A. Beer, and G. W. Hammett, Phys. Plasmas **2**, 2381 (1995).

[15] R. J. Hawryluk, V. Arunasalam, C. W. Barnes, M. Beer, M. Bell, et al., Plasma Phys. And Controlled Fusion, **33**, 1509 (1991)

[16] J. W. Connor, G. P. Maddison, H. R. Wilson, G. Corrigan, T. E. Stringer, F. Tibone, Plasma Phys. Control. Fusion **35**, 319 (1993)

[17] F. Tibone, J. W. Connor, T. E. Stringer, H. R. Wilson, Plasma Phys. Control. Fusion **36**, 473 (1994)

[18] B. A. Carreras, D. Newman, V. E. Lynch, P. H. Diamond, Plasma Phys. Reports **22**, 740 (1996)

[19] P. H. Diamond, T. S. Hahm, Phys. Plasmas **2**, 3640 (1995)

[20] P. C. Efthimion, C. W. Barnes, M. G. Bell, H. Biglari, N. Bretz, et al., Phys. Fluids B-Plasma Phys. **3**, 2315 (1991)

[21] D. R. Mikkelsen, S. D. Scott, W. Dorland, Phys. Plasmas, 4, 1362, (1997)

[22] M. Shimada, Nucl. Fusion **22** (1982) 643
[23] K. Lackner, R. Chodura, M. Kaufmann, J. Neuhauser, K. G. Rauh, and W. Schneider, Plasma Phys. Control. Fusion **26**, 105 (1984)
[24] G. F. Matthews, S. Allen, N. Asakura, J. Goetz, H. Guo, et al., J. Nucl. Mater. **241-243**, 450 (1997)
[25] J. Mandrekas, W. M. Stacey, and F. A. Kelly, Nucl. Fusion **37**, 1015 (1997)
[26] J. Mandrekas, W. M. Stacey, and F. Kelly, Nucl. Fusion **36**, 917 (1996)
[27] R. J. Goldston, Phys. Plasmas **3**, 1794 (1996)
[28] Weston M. Stacey, Plasma Phys. Control. Fusion **39**, 1245 (1997)
[29] G. Becker, Nucl. Fusion **35**, 39 (1995)
[30] D. E. Post, J. Nucl. Mater. **220-222**, 143 (1995)
[31] A. Kukushkin, H. D. Pacher, M. Baelmans, D. Coster, G. Janeschitz, et al., J. Nucl. Mater. **241-243**, 268 (1997)
[32] A. T. Ramsey, C. E. Bush, H. F. Dylla, D. K. Owens, C. S. Pitcher, M. A. Ulrickson, Nucl. Fusion **31**, 1811 (1991)
[33] M. Ulrickson, The JET Team, and The TFTR Team, J. Nucl. Mater. **176 & 177**, 44 (1990)
[34] U. Samm, G. Bertschinger, P. Bogen, J. D. Hey, E. Hintz, et al., Plasma Phys. Control. Fusion **35**, B167 (1993)
[35] A. Kallenbach, R. Dux, H.-S. Bosch, K. Buchl, ASDEX Upgrade, NI and ICRH Teams, Plasma Phys. Control. Fusion **38**, 2097 (1996)
[36] M. E. Fenstermacher, S. L. Allen, N. H. Brooks, D. A. Buchenauer, T. N. Carlstrom, et al., Phys. Plasmas **4**, 1761 (1997)
[37] K. Itami and the JT-60 Team, Plasma Phys. Control. Fusion **37**, A255 (1995)
[38] J. D. Strachan, Phys. Rev. Lett. **58**, 1004 (1987).
[39] D. E. Post, R. V. Jensen, C. B. Tartar, W. H. Grasberger, and W. A. Lokke, At. Dat. Nucl. Dat. Tables **20**, 397 (1977)
[40] H. F. Dylla, P. H. LaMarche, M. Ulrickson, R. J. Goldston, D. R. Heifetz, K. W. Hill, and A. T. Ramsey, Nucl. Fusion **27**, 1221 (1987)
[41] P. N. Yushimanov, Nucl. Fusion **30**, 1999 (1990).
[42] A. M. Messiaen, J. Ongena, U. Samm, B. Unterberg, P. E. Vandenplas, et al., Nucl. Fusion **34**, 825 (1994)
[43] J. D. Strachan, M. Bell, A. Janos, S. Kaye, S. Kilpatrick, et al., J. Nucl. Mater. **196-198**, 28 (1992)
[44] R. A. Hulse, Nucl. Technol./Fusion **3**, 259 (1983)

[45]B. C. Stratton, S. A. Cohen, F. P. Boody, C. E. Bush, R. J. Fonck, et al., Nucl. Fusion **27**, 1147 (1987)
[46] K. W. Hill, M. Bitter, N. L. Bretz, M. Diesso, P. C. Efthimion, et al., Nucl. Fusion **26**, 1131 (1986)
[47] M. Bitter, K. W. Hill, M. Zarnstorff, S. von Goeler, R. Hulse, et al., Phys. Rev. **A 32**, 3011 (1985)
[48] A. T. Ramsey and D. M. Manos, J. Nucl. Mater. **196-198**, 509 (1992)
[49] J. Schivell, Rev. Sci. Instrum. **56**, 972 (1985)
[50] J. Schivell, Rev. Sci. Instrum. **58**, 12 (1987)
[51] K. M. McGuire, C. W. Barnes, S. H. Batha, M. A. Beer, M. G. Bell, et al., *Plasma Physics and Controlled Nuclear Fusion Research*, 1996 (International Atomic Energy Agency, Vienna, 1997), Vol. 1, p. 19
[52] K. W. Hill, V. Arunasalam, M. G. Bell, M. Bitter, W. R. Blanchard, et al., in Proc. Eleventh International Conference on Plasma Physics and Controlled Nuclear Fusion Research, (Kyoto, Japan, November 1986) (International Atomic Energy Agency, Vienna, Austria, 1987) Vol **I**, p. 207, Paper IAEA-CN-47/A-IV-2
[53] H. F. Dylla, M. Ulrickson, M. G. Bell, D. K. Owens, D. Buchenauer, et al. J. Nucl. Mater. **162**, 128 (1989)
[54] K. M. McGuire, C. W. Barnes, S. H. Batha, M. A. Beer, M. G. Bell, et al., *Plasma Physics and Controlled Nuclear Fusion Research*, 1996 (International Atomic Energy Agency, Vienna, 1997), Vol. 1, p. 19
[55] Alan T. Ramsey and Stephen L. Turner, Rev. Sci. Instrum. **58**, 1211 (1987)
[56] K. Behringer, H. P. Summers, B. Denne, M. Forrest, and M. Stamp, Plasma Phys. Control. Fusion **31**, 2059 (1989)
[57] R. J. Hawryluk, in *Physics of Plasmas Close to Thermonuclear Conditions*, ed. B. Coppi *et al.* (Commission of the European Communities, Brussels, 1980), Vol. 1, p. 19.
[58] P. -H. Rebut, M. L. Watkins, D. J. Gambier, and D. Boucher, Phys. Fluids B **3**, 2209 (1991).

FIGURES

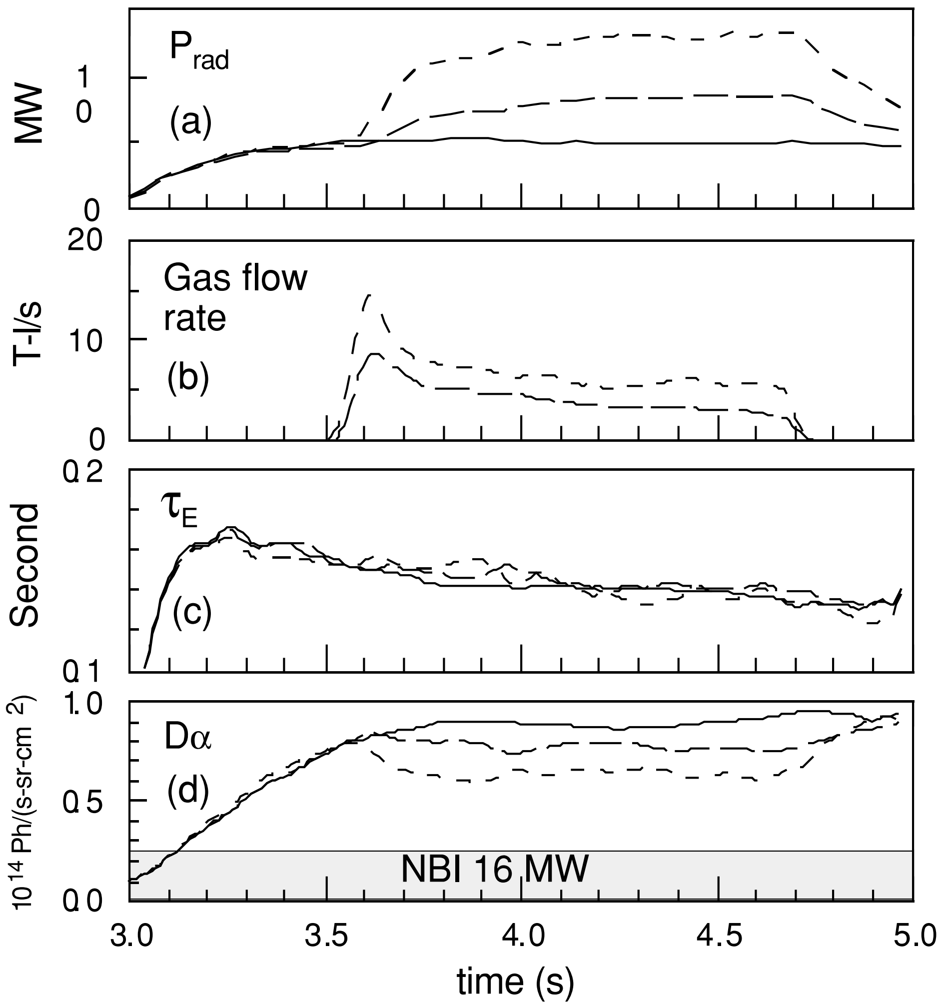

Figure 1 Time evolution of (a) Total radiated power, (b) xenon gas flow rate, (c) energy confinement time τ_E, and (d) Dα brightness for matched supershots with different requested radiated power fractions (dashed and long-dashed curves) and a reference shot without xenon puffing. The xenon puffing valve was feedback controlled on the radiated power fraction. The requested power fractions were 45% (long-dashed curves) and 75% (short dashed curves) of the total NB (Neutral-Beam) plus Ohmic heating power.

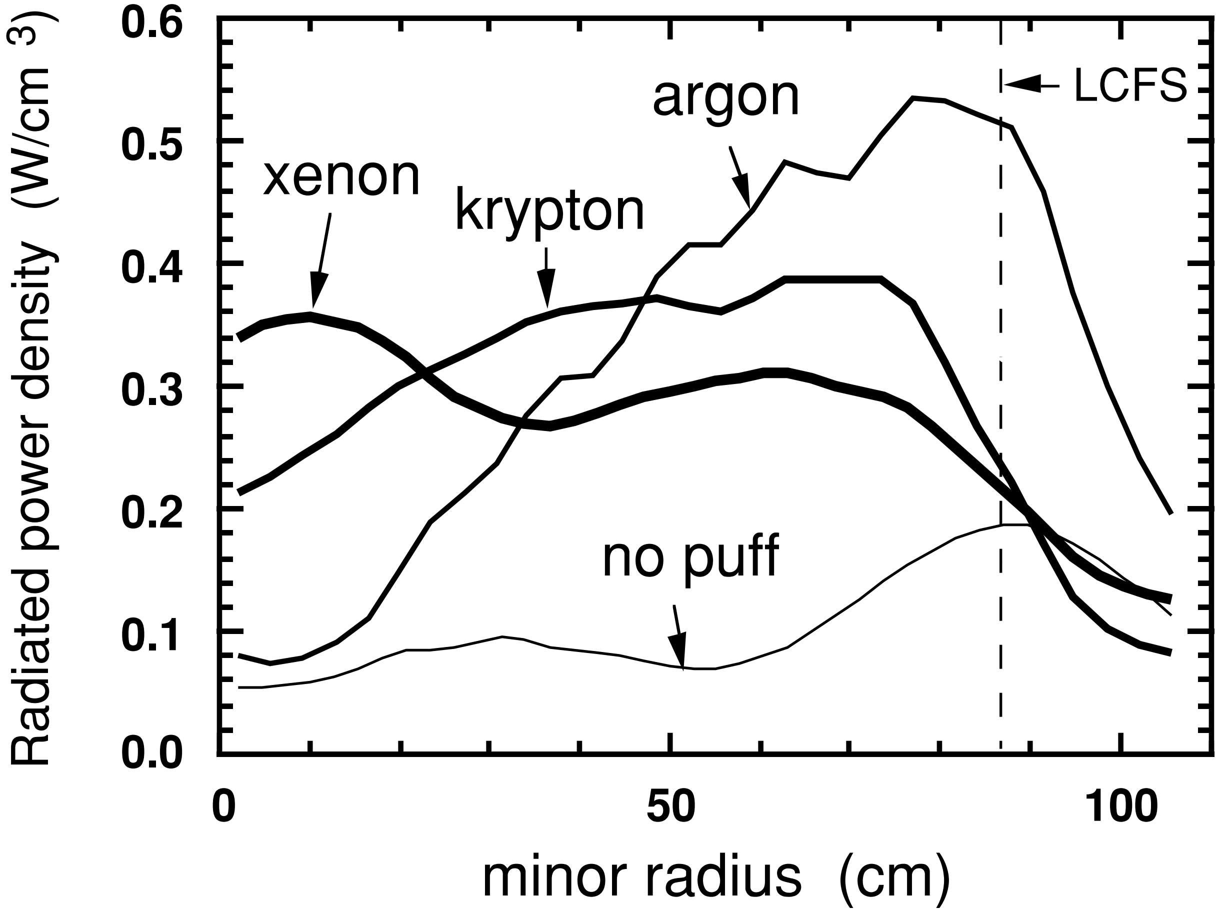

Figure 2 Measured radiated power density profiles for supershots with argon, krypton, and xenon gas puffs, and a matched shot with no gas puff for reference. The position of the last closed flux surface, LCFS, is indicated.

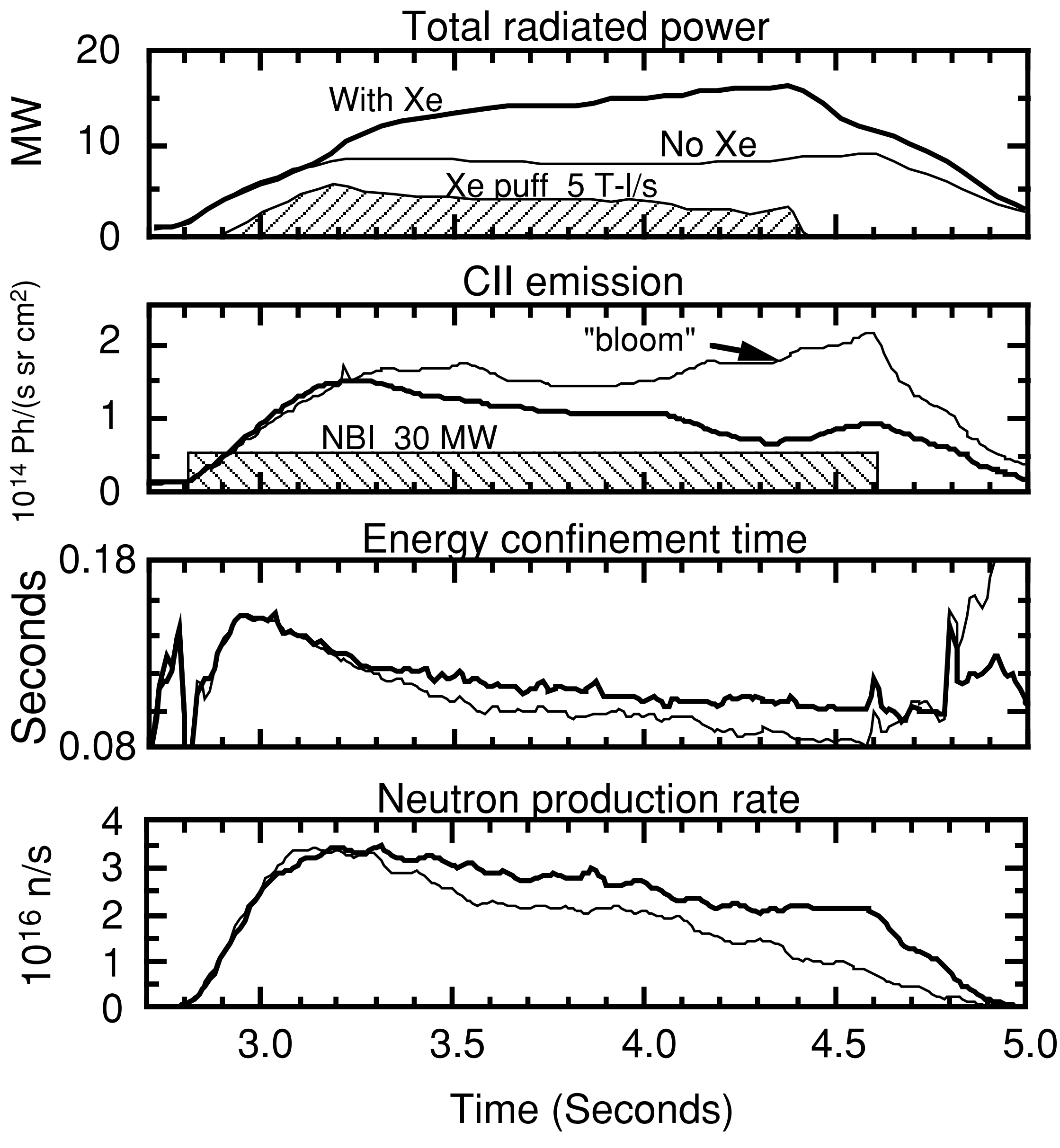

Figure 3 Time evolution of (a) Total radiated power, (b) CII brightness, (c) global energy confinement time, and (d) DD neutron production rate for two matched supershots. One shot (thin curves) had no impurity gas puffing, and the other (thick curves) had a xenon puff as illustrated by the boundary of the hatched curve shown in frame (a).

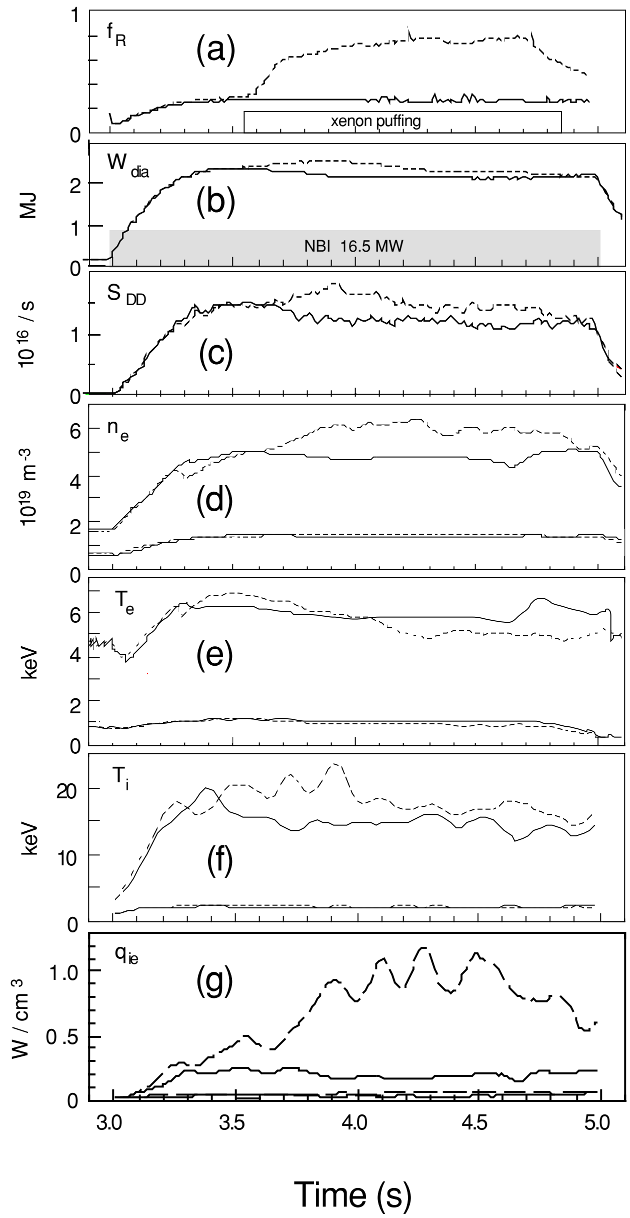

Figure 4 Time evolution of several plasma parameters for matched supershots with no impurity gas puffing (solid curves) and with xenon puffing (dashed curve, same shot as short-dashed curve of Fig. 1). The parameters are (a) radiated power fraction, (b) plasma stored energy, (c) DD neutron production rate, (d) central (upper solid and dashed curves) and (near) edge (lower solid and dashed curves) electron density, (e) central and edge electron temperature, (f) central and edge ion temperature, and (g) central and edge ion-electron equilibration power as calculated by the TRANSP code. The xenon puffing period is illustrated in frame (a) (or in frame b of Fig. 1), and the neutral-beam heating was 16.5 MW as illustrated in frame (b).

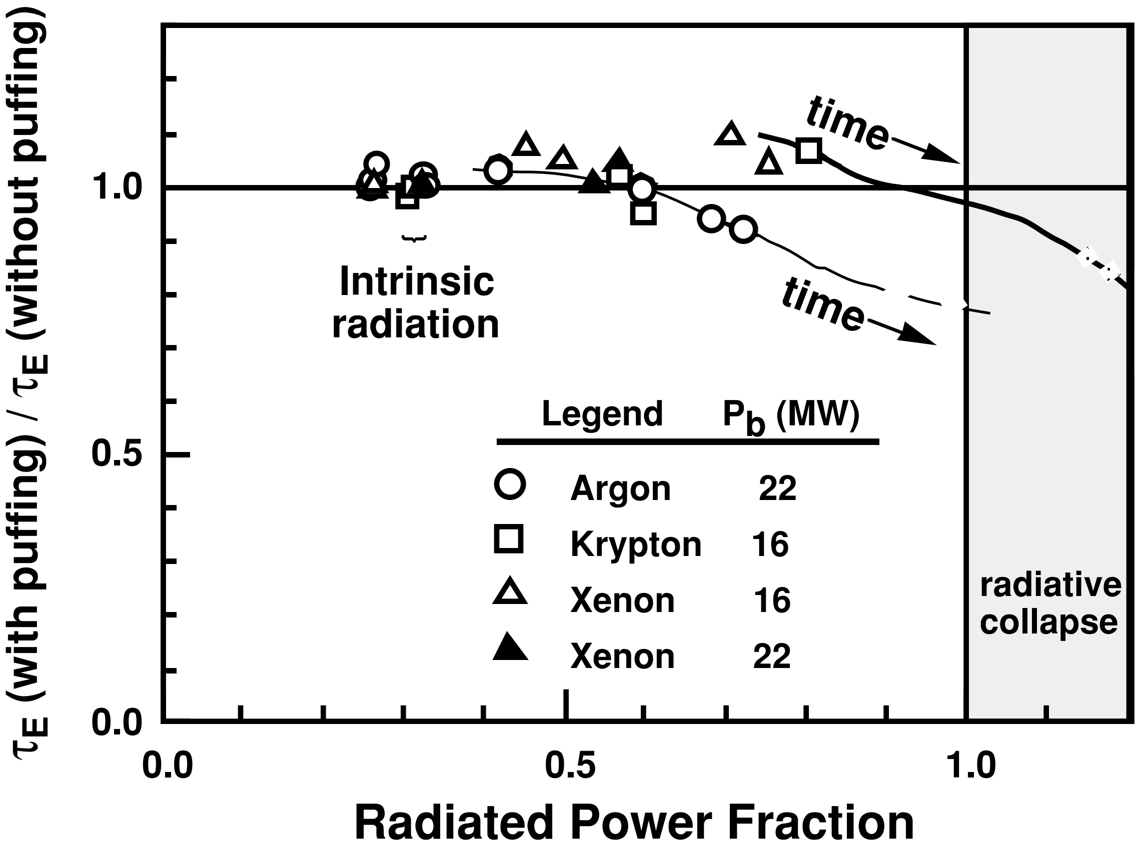

Figure 5 Ratio of global energy confinement time in discharges with high-Z impurity puffing to that in matched reference discharges as a function of radiated power fraction. The solid lines illustrate the time evolution of individual discharges that ultimately suffered radiative collapse; the dashed lines represent time periods when dW_{tot}/dt exceeds 15% of the total input power.

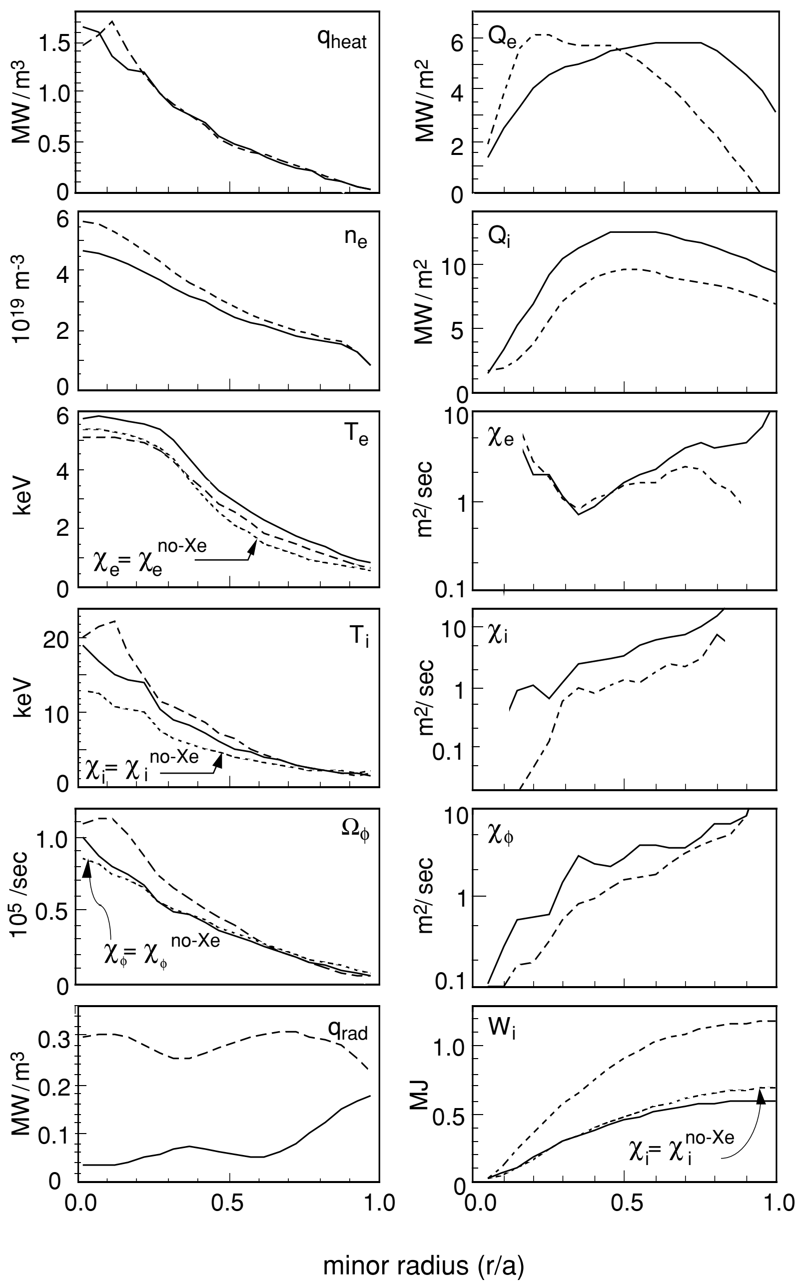

Figure 6 Radial profiles of several parameters at a fixed time (near 4.0 s) for the two shots of Fig. 4. The shots represented by the solid curves had no impurity gas puffing, and those represented by the dashed curves had xenon puffing. The curves are either smoothed measured parameters (n_e, T_e, T_i, q_{rad}) used as input data for the TRANSP code, or quantities calculated by TRANSP. The short-dashed curves in the frames for T_e, T_i, Ω_ϕ, and W_i are taken from predictive runs of TRANSP assuming that the respective transport coefficients in the xenon-puff shot were the same as those in the no-puff shot.